

Current Biology, Volume 29

Supplemental Information

**Alternative Mechanisms for Fast Na⁺/Ca²⁺
Signaling in Eukaryotes via a Novel Class
of Single-Domain Voltage-Gated Channels**

Katherine E. Helliwell, Abdul Chrachri, Julie A. Koester, Susan Wharam, Frédéric Verret, Alison R. Taylor, Glen L. Wheeler, and Colin Brownlee

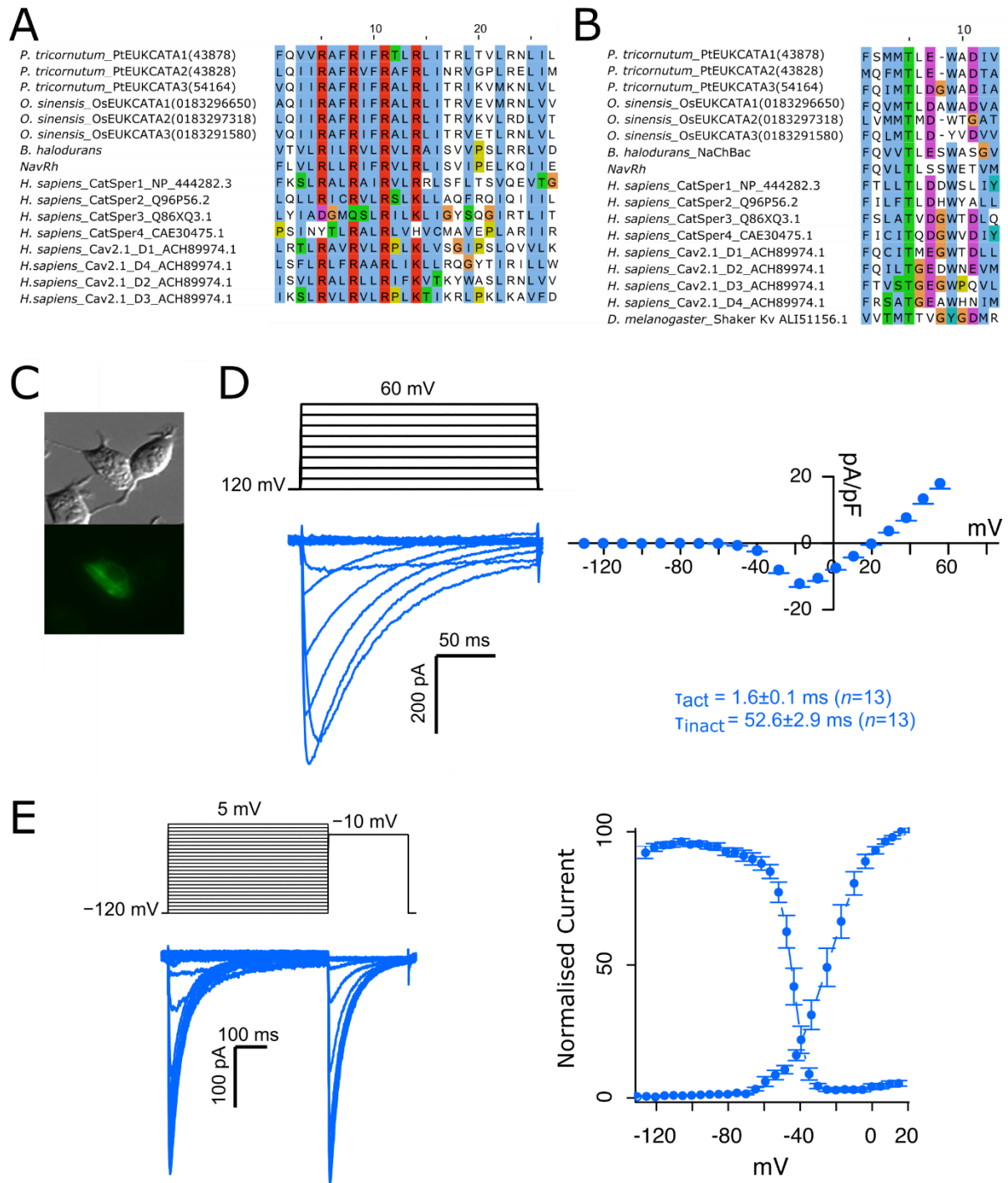


Figure S1. Diatom EukCatAs exhibit a predicted voltage-sensing domain and selectivity filter, and OsEUKCATA1 expressed in HEK293 cells exhibits rapid activation and inactivation kinetics resembling those of *O. sinensis* action potentials (related to Figure 1 & 2; Table S1 and S2; Data S1). A. Alignment of the voltage-sensing domain of diatom EukCatAs (including OsEUKCATA1 and PtEUKCATA1) compared to other voltage-gated channels. The presence of multiple positively charged Arg residues are indicated. The region shown corresponds to amino acids 109-135 of *Bacillus halodurans* C-125 NaChBac

(BAB05220.1 BH1501). The CatSpers are relatively weakly voltage-gated, with subunits three and four possessing fewer Arg residues in this region. **B.** Alignment of the selectivity filter of EukCats (corresponding to amino acids 185 to 197 of NaChBac) to voltage-gated Ca^{2+} , Na^{+} and K^{+} channels. **C.** DIC and GFP fluorescence image confirming expression of PtEUKCATA1-GFP fusion in a transfected HEK293 cell. **D.** Representative currents (I) for OsEUKCATA1 with averaged current-voltage (IV) curves (right), where I was normalized to cell capacitance ($n=24$). **E.** Representative traces for steady state inactivation (left) and normalized currents (right), where activation is represented by tail current analysis. Boltzmann fitted functions yielded $V_{0.5}$ of inactivation of -45.11 ± 0.2 mV ($n=12$) and the $V_{0.5}$ of activation of -23.8 ± 0.2 mV ($n=12$). OsEUKCATA1 exhibited rapid kinetics: $\tau_{\text{activation}}$ and $\tau_{\text{inactivation}}$ time constants (measured at -10 mV) were 1.6 ± 0.1 ms (OsEUKCATA1), and 52.6 ± 2.9 ms (OsEUKCATA1), respectively (**Table S1**). These are comparable to 4D- Ca_v/Na_v s and closely resemble those of the *O. sinensis* action potentials (**Figure 1A**) [S1].

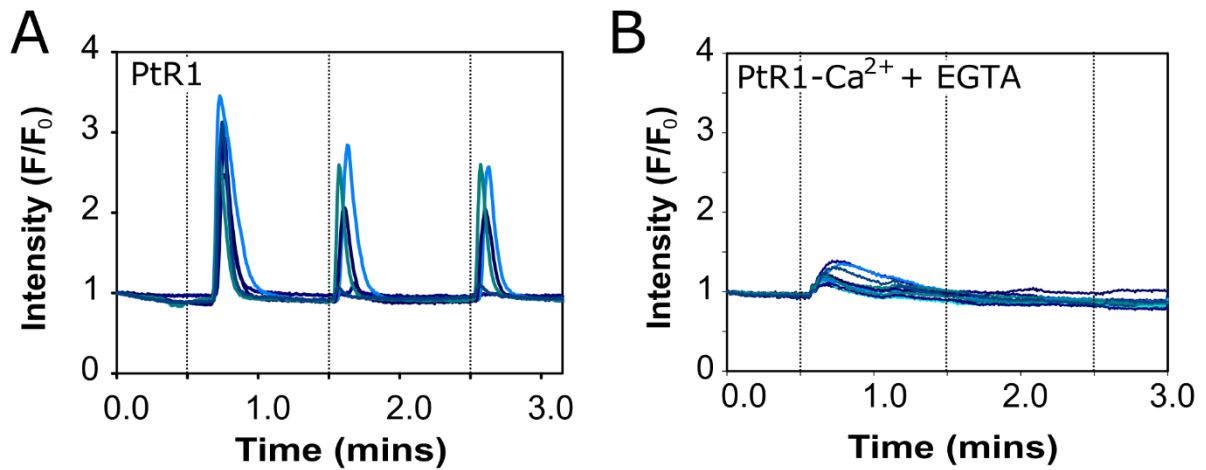


Figure S2. Transgenic *P. tricornutum* stably expressing the intensimetric fluorescent Ca²⁺ indicator R-GECO (line PtR1) exhibits robust [Ca²⁺]_{cyt} elevations in response to hypo-osmotic shock (related to Figure 3). A. Representative traces of Ca²⁺ responses (F/F₀) over time for PtR1 cells exposed to three sequential 30 s hypo-osmotic shocks with 90% ASW diluted 10% with deionised water. Hypo-osmotic shocks were elicited at 30, 90 and 150 s (dashed lines) and between each shock cells were returned to standard ASW medium before the next treatment. **B.** as in (A) but in ASW diluted 50% with deionised water –Ca²⁺ +200 μM EGTA. Representative traces are shown from a total of 5 cells and 11 cells, respectively.

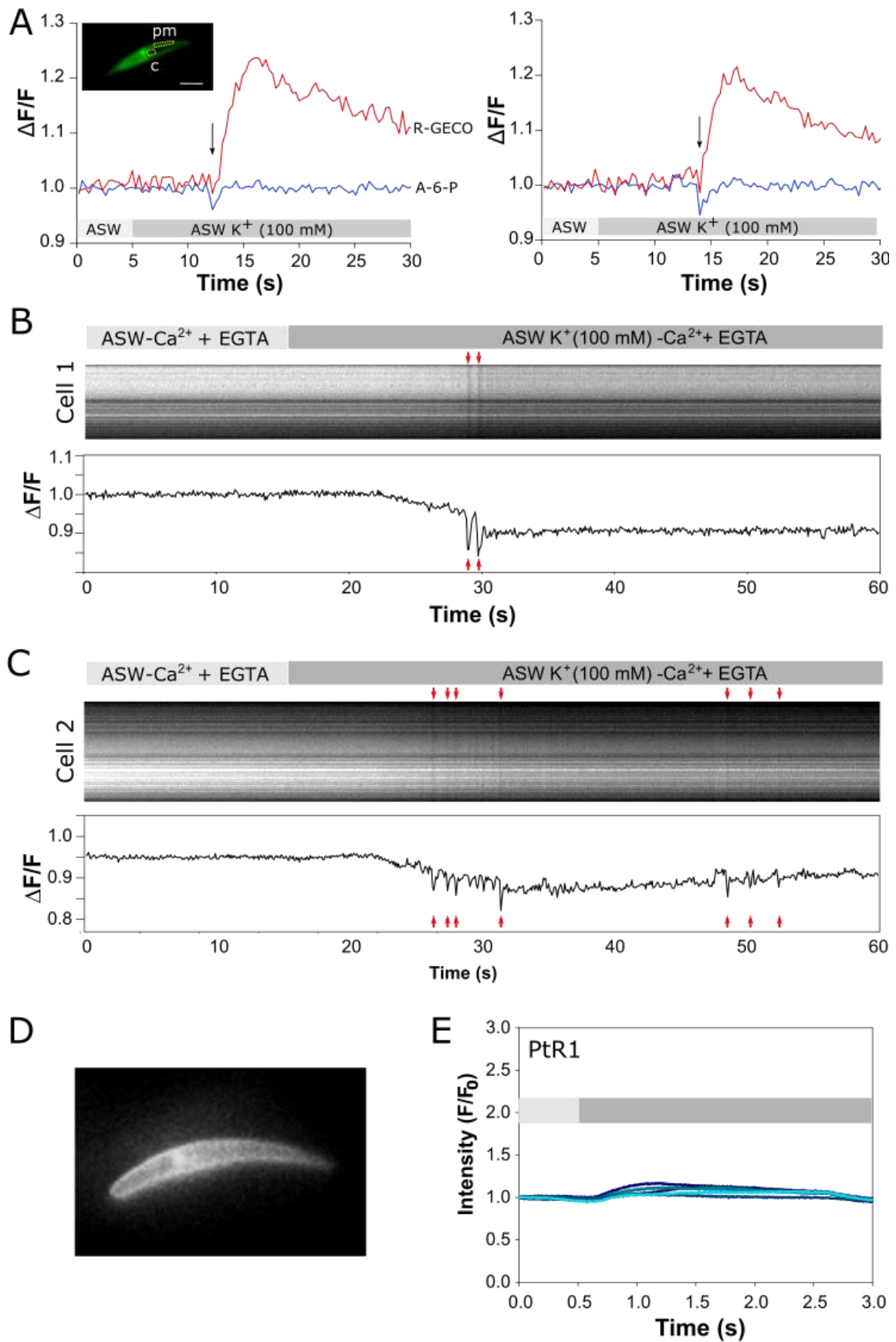


Figure S3. Rapid depolarisation-activated action potentials are immediately followed by a $[Ca^{2+}]_{\text{cyt}}$ elevation, but are not dependent on external Ca^{2+} (related to Figure 3). A.

Simultaneous determination of membrane potential and cytosolic Ca^{2+} . PtR1 cells expressing R-GECO in the cytosol were loaded with the membrane potential dye Annine-6-Plus. Specific regions of interest were used to measure fluorescence in the plasma membrane (pm) and cytosol (c) (inset). Cells were stimulated with 100 mM K^+ to induce membrane depolarisation. Rapid depolarisation events (arrowed) directly preceded the $[\text{Ca}^{2+}]_{\text{cyt}}$ elevation. The A-6-P trace was generated by dividing fluorescence in each frame by a rolling median of the ten neighbouring frames to aid visualisation of rapid changes in fluorescence. A threshold decrease in fluorescence of $>3\%$ (>4 SD of baseline fluorescence) was used to identify depolarisation events. The Ca^{2+} trace was generated by dividing normalised R-GECO fluorescence by normalised A-6-P fluorescence to compensate for background A-6-P fluorescence in the cytosolic region. Two representative cells are shown ($n=4$). Bar= 5 μm . **B.** Kymograph from a WT A-6-P stained cell following exposure to ASW + 100 mM K^+ - Ca^{2+} + 200 μM EGTA (after 15 s for 45 s) (12.5 frames/s). The kymograph represents changes in fluorescence in the plasma membrane along the length of the cell. Corresponding data for $\Delta F/F$ over time (s) is plotted below. A further example is shown in (C). In the absence of external Ca^{2+} (+200 μM EGTA) multiple transient decreases in fluorescence (arrowed) are observed following the initial depolarisation in response 100 mM K^+ . **D.** An epifluorescence microscopy image of a WT *Phaeodactylum tricornutum* cell stained with the voltage-sensing dye Annine-6-Plus (A-6-P) used to generate kymograph shown in (C). **E.** Change in fluorescence intensity of R-GECO in 6 representative PtR1 cells exposed to 100 mM K^+ - Ca^{2+} + 200 μM EGTA (following pre-perfusion with ASW - Ca^{2+} +200 μM EGTA) is shown (the experiment was repeated on three independent occasions, n cells =25, with similar results).

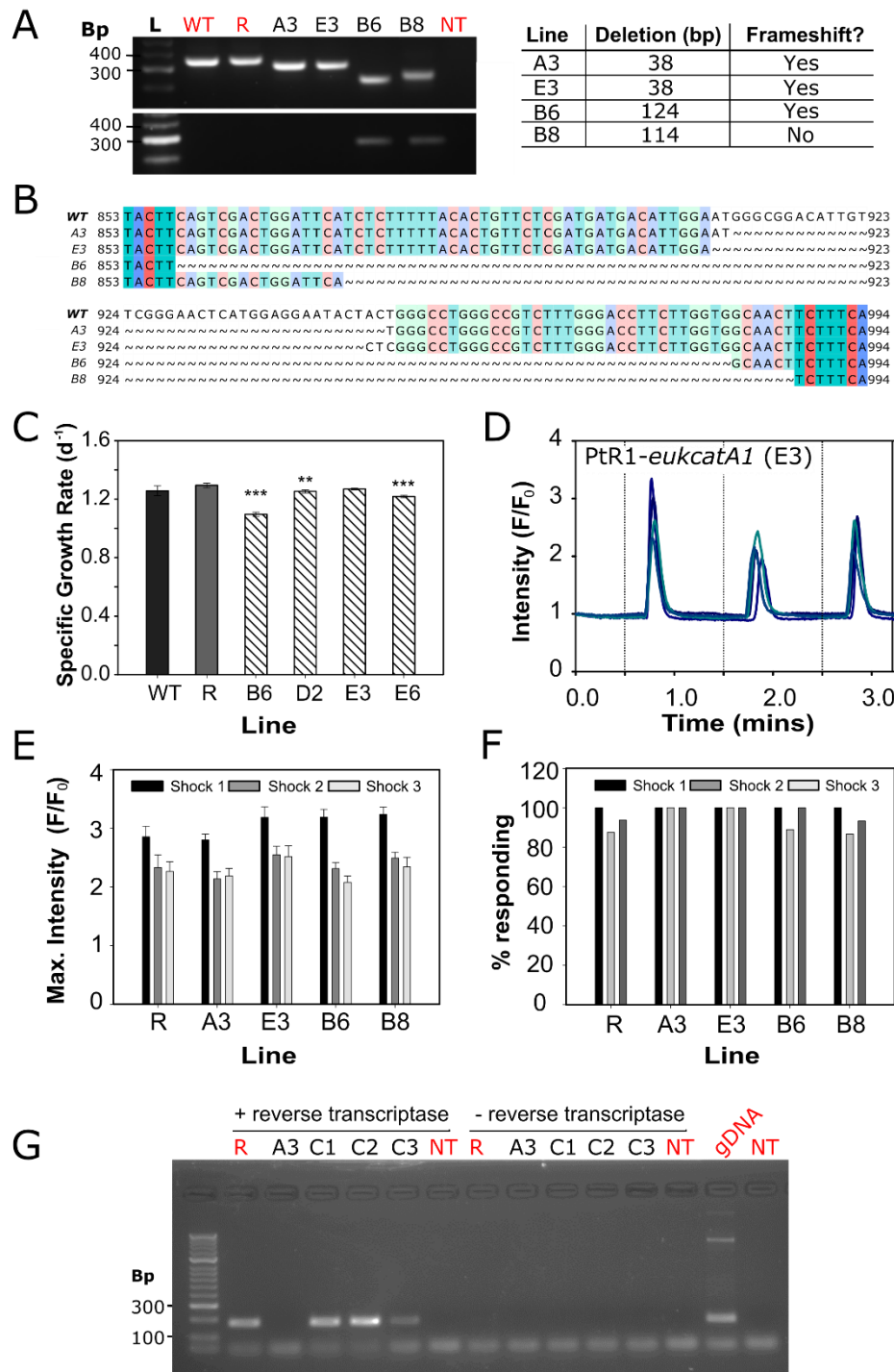


Figure S4. Biallelic *PtR1-eukcatA1* mutants exhibit a modest reduction in growth rate and are unimpaired in Ca^{2+} -signalling responses to hypo-osmotic shock (related to Figure 3 and 4). A. Bi-allelic *PteukcatA1* mutants were generated using CRISPR-Cas9 with two guide RNAs (sgRNAs) targeted approximately 50 bp apart to span the pore region encoded by the *PtEUKCATA1* gene. PCR amplification of *PtEUKCATA1* from genomic DNA from four independent mutant lines (A3, E3, B6, B8) using primers flanking the two sgRNAs. The

expected product size for WT *PtEUKCATA1* is 350 bp. The smaller products indicate deletions in this region of the genome of mutants (upper panel). Lower gel shows amplification of Cas9 gene: transgene has been lost from mutants A3 and E3. Key: L, ladder; WT, wild type; R, PtR1 (R-GECO) line; NT, no template control. Summary of deletions in independent mutant lines is also shown. **B.** Multiple sequence alignment of *PtEUKCATA1* following sequencing of the PCR products shown in (A). The region of excision varies between lines and extends beyond the original target site of each guide RNA (**methods**). **C.** Specific growth rate of WT fusiform cultures of *P. tricornutum*, PtR1 alongside 4 independent PtR1-*eukcatA1* mutants in liquid f/2 media ($n=3$). **D.** Representative traces of Ca^{2+} responses for PtR1-*eukcatA1* mutant E3 (intensity of fluorescence) over time exposed to three sequential hypo-osmotic shocks with diluted ASW (90%) as in **Figure S2A**. **E.** Mean maximum intensity of responses to successive shocks for multiple cells over 3 independent replicate experiments per line (error bars, SEM; at least 10 cells were analysed per line, and only those cells that responded are included in analysis) including PtR1 and four independent PtR1-*eukcatA1* mutants (A3, E3, B6, and B8). **F.** Proportion of cells that respond to hypo-osmotic shock (only cells exhibiting $[Ca^{2+}]_{cyt}$ elevations were used for comparison). **G.** Complemented PtR1-*eukcatA1* mutant A3 lines express the WT *PtEUKCATA1* transcript. Reverse transcriptase PCR on cDNA synthesised from PtR1 (R), mutant line A3 (A3), the three complemented lines (C1-C3), and no template (NT) control. Cultures were sampled four days after inoculation. Primers used were designed to the *PtEUKCATA1* gene and the expected product size was 176 bp (note: the reverse primer targets the deletion site of the *ptEUKCATA1* gene in the A3 mutant, and therefore a product will only be amplified in lines containing the WT gene i.e. R, C1, C2, and C3). The primer sequences were as follows: TTTTGGTGCTTATTCTCTACGTC (forward) and TTCCTCCATGAGTTCCCGAA (reverse).

	NaChBac [S2]	PtEUKCATA1	OsEUKCATA1
	<i>Bacillus halodurans</i>	<i>Phaeodactylum tricornutum</i>	<i>Odontella sinensis</i>
SF	TLESWA	TLE-WAD	TLDAWAD
Voltage of half activation (mV)	-48.1±1.5 (n=10)	-18.7±0.4 (n=14)	-23.8±0.2 (n=12)
Voltage of half steady-state inactivation	-52.7±0.3 (n=20)	-56.5±1.6 (n=17)	-45.1±0.2 (n=12)
τ activation (ms)	12.9 ± 0.4	9.2±1.9 (measured at -10 mv) (n=26)	1.6±0.1 (measured at -10 mv) (n=13)
τ inactivation (ms)	166 ± 13	33.0±5.8 measured (at -10 mv) (n=26)	52.6±2.9 (measured at -10 mv) (n=13)
τ of recovery of inactivation (ms)	650±33.5 (n=3)	650±33.5 (n=3)	183±6.9 (n=15)

Table S1. Summary of kinetic properties and pharmacology of PtEUKCATA1 and OsEUKCATA1 (related to Figure 2 and Figure S1). Number of cells (*n*) examined is indicated.

	E1	P	E2	E3	E4
NaCl	140	10	140	-	-
KCl	4	-	4	4	4
MgCl₂	1	1	1	1	1
CaCl₂	5	1	-	30	-
CsCl	-	-	5	5	5
CsF	-	130	-	-	-
BaCl₂	-	-	-	-	30
HEPES	10	10	10	10	10
NMDG	-	-	-	140	140
TEA-Cl	-	5	-	-	-
EGTA	-	10	-	-	-
Glucose	5	-	-	-	-
D-Sorbitol	5	-	-	-	-
pH	7.4	7.2	7.4	7.4	7.4
	NaOH	CsOH	CsOH	CsOH	CsOH

Table S2. Composition of electrophysiology solutions (mM) (related to Figure 2). NMDG, N-methyl-D-glutamine; E: Extracellular solution; P: pipette solution; E1: standard extracellular solution; E2: 0 CaCl₂ (-Ca²⁺); E3: 0 NaCl₂ with 30 mM CaCl₂ (-Na⁺); E4: 0 NaCl₂ with 30 mM BaCl₂ (+Ba²⁺). For OsEUKCATA1: 10 mM glucose was included, but not MgCl₂ and KCl, and the concentration of NMDG in E3 and E4 was 95 mM.

Supplemental References

- [S1] Taylor, A.R. (2009). A Fast Na⁺/Ca²⁺-based action potential in a marine diatom. *PLoS One* 4, e4966.
- [S2] Ren, D., Navarro, B., Xu, H., Yue, L., Shi, Q., and Clapham, D.E. (2001). A prokaryotic voltage-gated sodium channel. *Science* 294, 2372–5.
- [S3] Verret, F., Wheeler, G., Taylor, A.R., Farnham, G., and Brownlee, C. (2010). Calcium channels in photosynthetic eukaryotes: implications for evolution of calcium-based signalling. *New Phytol.* 187, 23–43.
- [S4] Cai, X., Wang, X., and Clapham, D.E. (2014). Early evolution of the eukaryotic Ca²⁺ signaling machinery: conservation of the CatSper channel complex. *Mol. Biol. Evol.* 31, 2735–2740.